Modal PD state active control applied to a simplified string instrument

Authors:
Simon Benacchio[1], Baptiste Chomette[2,3], Adrien Mamou-Mani[1] and François Ollivier[2,3]

[1] UMR STMS IRCAM-CNRS-UPMC, 1 place Igor Stravinsky 75004 Paris, France
[2] CNRS, UMR 7190, Institut Jean Le Rond d'Alembert, F-75005 Paris, France
[3] UPMC, Université Pierre et Marie Curie 06, Institut Jean Le Rond d'Alembert F-75005 Paris, France

Corresponding author:
Simon Benacchio (benacchio@ircam.fr)

Abstract

This study proposes an application of modal active control on musical string instruments. Its aim is to control the modal parameters of the soundboard in order to modify the sound of the instrument. Using both state and derivative state modal control, a method is given, from the modeling of the active structure through to the design of the control system. Issues such as the identification of the structure's characteristics or the stability of the control system are dealt with for this original control method. Then, this technique is applied on a model of a simplified string instrument soundboard. Time simulations are conducted to study its effect on the instrument vibration. They show that, thanks to soundboard modal active control, it is possible to modify the amplitude of the sound harmonics to change the timbre as well as the sound level of the instrument.

1 Introduction

One of the usual aims of active control is to decrease vibration. A lot of techniques can be used to reach this goal (Nelson and Elliott, 1992; Fuller et al., 1996). For some of them, the control is colocated in the physical space (Preumont, 2001) while for others it is based on a linear description of the controlled system using a state space model (Richards, 1979; Meirovitch, 1990; Franklin et al., 1994). Combined with the observers theory (Luenberger, 1971), these last techniques are convenient for modifying the state variables of a system. The automatic control community often applies and improves these techniques on complex systems. One of these is the derivative state space control which is based on the derivative state of the system. However, the use of this technique brings new issues such as the stability of the system controlled thanks to an acceleration measurement (Abdelaziz and Valàšek, 2003; Abdelaziz, 2012). Another example of a method used for automatic control issues, is the proportional and derivative (PD) state space feedback which uses not only the state of a structure but also its derivative state (Dai, 1989).

As the active control is a specific part of automatic control, a lot of these methods have been used in order to cancel noise or structural vibration (Lhuillier et al., 2008). For instance, a particular case of the state space control methods, called the modal active control (Gawronski, 1998), is known as a very convenient way to modify the modal characteristics of a structure (Chomette et al., 2008). In this method, a model of the structure is required and can be found thanks to identification techniques (Richardson and Formenti, 1982). Some estimation algorithms used for this identification step enable the modeling of the structure by using experimental data measured directly between the actuators and the sensors which are used for the control (Chesné et al., 2013). Then, controller and observer gains have to be found to reach the control target, ensuring the stability of the system. A pole placement or a Linear Quadratic Gaussian (LQR) algorithm can be used (Abdelaziz and Valàšek, 2003; Franklin et al., 1994). Another important issue in a control system is the choice of the transducers' characteristics used as actuators and sensors. The use of piezoelectric patches is a good way to control the vibration of a structure. A lot of tools have been developped to estimate the effect of the piezoelectric patches on the vibration of the structure. The optimal location of the transducers can be found using the Hać and Liu criterion (Hać and Liu, 1993). Numerical models using the finite element method can also be developped to choose the characteristics of these transducers (Piefort and Preumont, 2000).

All these enhancements have led active control to not only be used to cancel the vibration but also to modify it. For example, some active control methods have already been applied on percussions and on string instruments (Boutin, 2011; Boutin and Besnainou, 2012; Griffin,

1995; Berdahl et al., 2006; Berdahl and Smith III, 2007). Indeed, a very simple model of a bowed string instrument is to consider it as a resonant filters system (Mathews and Kohut, 1973). However, only bowed string instruments where the coupling phenomenon between the string and the soundboard is neglected can be modeled in such a way. In this case, the radiating structure is the soundboard. It is considered to be the resonant filters part with its own mechanical properties and excited by the bowed string signal. The sound radiated by this simple model is harmonic in the frequency domain. Its pitch is forced by the partials' frequencies of the string signal whereas its timbre is the result of the amplitude modulation of its partials by the vibration modes of the soundboard. Moreover, the modal amplitudes of the soundboard are also important factors for the radiated sound since they have an influence on the average mobility or in other words on the loudness of the instruments (Richardson, 2002; Jansson, 2002). According to this simple model, the control of the soundboard modal parameters can modify the timbre and the sound loudness of a bowed string intrument. The application of these modifications without changing the construction materials of an instrument is a real issue for instrument makers. Thanks to this possibility, they could modify the sound of an instrument without changing its weight or its solidity.
The following study proposes an original method combining the modal active control and the PD state space approach in order to modify the modal frequencies, damping and amplitudes of a structure. The principle of this technique is given using a simple example of one mode. The first step is the modeling of the structure in the state space. Then, an identification method is applied to estimate modal parameters of the smart-structure. A double pole placement method based on a recursive algorithm and a usual pole placement method is then used in order to find the controller gains ensuring the stability of the system. This method is then applied on a simplified soundboard of a string instrument. Thanks to the soundboard control, the very perceptible partials of the radiated sound are decided to be controlled. A numerical model is used to find the optimal location of the transducers on the experimental setup. Finally, the effects of the control on a bowed string signal are numerically demonstrated using experimental data. The results of these simulations are presented and discussed in the last section.

2 Mechanical modeling

2.1 Modal state space modeling of the active structure

The main advantage of the modal active control is to target the control exclusively on the vibration modes of interest. This method is based on the state space approach using a system description by first order equations. In the case of modal control, the equations describing the system which are functions of the state variables of the structure, are found thanks to a modal decomposition. The dynamics of the k^{th} mode of vibration of the structure without external load is given by

$$\ddot{q}_k(t) + 2\xi_k\omega_k\dot{q}_k(t) + \omega_k^2 q_k(t) = 0, \tag{1}$$

where ξ_k and ω_k are the modal damping and modal frequency of the described mode and q_k, $\dot{q}_k$ and $\ddot{q}_k$ are the modal displacement, speed and acceleration respectively. For a system including n modes, $k = 1, ..., n$.

[Figure 1 about here.]

In this case, the dynamic of the controlled structure shown in Figure 1 may be described in the state space by a set of first order linear differential equations

$$\begin{cases} \dot{\mathbf{X}}(t) = \mathbf{A}\mathbf{X}(t) + \mathbf{B}u(t) + \mathbf{G}w(t) \\ y(t) = \mathbf{C}\mathbf{X}(t) \end{cases}, \tag{2}$$

where $\mathbf{X}(t)$ is the state vector and $u(t)$, $y(t)$ and $w(t)$ are the control, measured and disturbance signal respectively. $\mathbf{A}$, $\mathbf{B}$, $\mathbf{C}$ and $\mathbf{G}$ are the structure, the input, the output and the disturbance signal input matrices respectively. For a usual state space control system in the modal basis and for a multi-input/multi-output (MIMO) system their expressions are

$$\mathbf{X}(t) = \begin{pmatrix} \mathbf{q}(t) \\ \dot{\mathbf{q}}(t) \end{pmatrix}, \tag{3}$$

$$\mathbf{A} = \begin{pmatrix} \mathbf{0}_{n,n} & \mathbf{Id}_{n,n} \\ -diag\left({\omega_k}^2\right) & -diag\left(2\xi_k\omega_k\right) \end{pmatrix}, \tag{4}$$

$$\mathbf{B} = \begin{pmatrix} 0 & \cdots & 0 \\ \vdots & & \vdots \\ 0 & \cdots & 0 \\ \Pi_1^a(P_1) & \cdots & \Pi_1^a(P_p) \\ \vdots & & \vdots \\ \Pi_n^a(P_1) & \cdots & \Pi_n^a(P_p) \end{pmatrix} = \begin{pmatrix} \mathbf{0}_{n,1} & \cdots & \mathbf{0}_{n,1} \\ \mathbf{\Pi}^a(P_1) & \cdots & \mathbf{\Pi}^a(P_p) \end{pmatrix}, \tag{5}$$

$$\mathbf{C} = \begin{pmatrix} \Pi_1^s(Q_1) & \cdots & \Pi_n^s(Q_1) & 0 & \cdots & 0 \\ \vdots & & \vdots & \vdots & & \vdots \\ \Pi_1^s(Q_q) & \cdots & \Pi_n^s(Q_q) & 0 & \cdots & 0 \end{pmatrix} = \begin{pmatrix} \mathbf{\Pi}^s(Q_1) & \mathbf{0}_{1,n} \\ \vdots & \vdots \\ \mathbf{\Pi}^s(Q_q) & \mathbf{0}_{1,n} \end{pmatrix}, \tag{6}$$

where P_i and Q_j denote the positions on the structure of the i^{th} actuator and j^{th} sensor. The elements $\Pi_k^a(P_i)$ and $\Pi_k^s(Q_j)$ are the coefficients in modal coordinates of the electromechanical coupling vectors $\mathbf{\Pi}^a(P_i)$ and $\mathbf{\Pi}^s(Q_j)$ of actuators and sensors respectively.
In this study, the control system is based on a single-input/single-output (SISO) system. That means that only one actuator and one sensor are used for the control. Consequently, $\mathbf{B}$ and $\mathbf{C}$ are one column and one row matrices respectively. As $\mathbf{B}$ and $\mathbf{C}$ are vectors, the positions of the actuator and sensor P_1 and Q_1 are omitted later. The elements of the electromechanical coupling vectors $\mathbf{\Pi}^a$ and $\mathbf{\Pi}^s$ are denoted Π_k^a and Π_k^s respectively.
These state matrices have to be filled out with the studied structure's characteristics to design the control system. In the section 2.2, an identification step is used to find the components of these matrices.

2.2 State model based on rational fraction polynomial identification

In the majority of cases, the actuator and the sensor modal parameters cannot be easily measured, particularly in the case of piezoelectric transducers with low electromechanical coupling coefficient. Furthermore, if the structure material is sensitive to external conditions, time can modify the modal frequencies and dampings of the structure, which are used to fill out state matrices. In this case, a good alternative is to use the Rational Fraction Polynomial (RFP) algorithm (Richardson and Formenti, 1982) to identify the state model $(\mathbf{A}, \mathbf{B}, \mathbf{C})$ used

by the control system. Indeed, this identification method can provide the characteristics used to fill out the state matrices using a simple transfer function between the actuator and the sensor. The RFP algorithm is based on the partial fraction form which can be written for n modes

$$H(s) = \sum_{k=1}^{n} \left(\frac{r_k}{s - p_k} + \frac{r_k^*}{s - p_k^*} \right), \tag{7}$$

where p_k and r_k are the poles and the residues of the system respectively, $s = j\omega$ is the Laplace variable and * denotes the conjugate. (7) can be expressed using the polynomial fraction form

$$H(s) = \sum_{k=1}^{n} \frac{A_k + B_k\, s}{s^2 - 2\mathcal{R}e(p_k)\, s + |p_k|^2}, \tag{8}$$

where A_k and B_k can be developed as functions of poles and residues

$$A_k = -2\left[\mathcal{R}e(p_k)\,\mathcal{R}e(r_k) + \mathcal{I}m(p_k)\,\mathcal{I}m(r_k)\right], \tag{9}$$

$$B_k = 2\,\mathcal{R}e(r_k). \tag{10}$$

In the case of piezoelectric transducers, the transfer function between one actuator and one sensor can be written as

$$H(j\omega) = \sum_{k=1}^{n} \frac{\Pi_k^a\, \Pi_k^s}{{\omega_k}^2 - \omega^2 + 2j\xi_k\omega_k\omega}, \tag{11}$$

where ω_k and ξ_k are the natural frequency and the modal damping respectively. Assuming small modal dampings and diagonal damping matrix, the modal parameters can be obtained using (8) and (11)

$$\omega_k = |p_k|,\ \xi_k = -\frac{\mathcal{R}e(p_k)}{|p_k|}, \tag{12}$$

$$\Pi_k^a\, \Pi_k^s = A_k + j\omega B_k \approx A_k. \tag{13}$$

Assuming that the total contribution of actuator and sensor is contained in vector $\mathbf{B}$ and that the non-zero elements of vector $\mathbf{C}$ are equal to the unit, (5) and (6) can be written using the identified modal parameters

$$\mathbf{B} = \begin{pmatrix} \mathbf{0}_{n,1} \\ \mathbf{\Pi}^a \cdot \mathbf{\Pi}^{st} \end{pmatrix}, \mathbf{C} = \begin{pmatrix} \mathbf{1}_{1,n} & \mathbf{0}_{1,n} \end{pmatrix}, \tag{14}$$

where $\cdot$ denotes the Hadamard product and ^{t} the transpose.
This identified state model is then used below to design the control system.

2.3 Design of the control system

2.3.1 Design of the controller

To the knowledge of the authors, the active control of vibration is rarely used to modify the modal amplitude of a structure. The control usually targets modal damping factors and frequencies of the structure. Althought the idea to control the modal amplitudes of a structure is not new (Boutin, 2011; Lhuillier et al., 2008), no theoretical criterion is given to ensure the stability of such a control system. In this section, a method is proposed to control the amplitude of a mode without changing its damping and frequency. Such a modification is

possible if the control signal $u(t)$ used to reach the new modal state of the control structure is built with two vector gains as in (15) and in the feedback loop of the Figure 2.

$$u(t) = -\mathbf{K}_1\mathbf{X}(t) - \mathbf{K}_2\dot{\mathbf{X}}(t). \tag{15}$$

[Figure 2 about here.]

Let's study the effect of this control on one mode. Its transfer function without control can be written as

$$\frac{Q_k}{F_k} = \frac{1}{(\omega_k^2 - \omega^2) + 2j\xi_k\omega_k\omega}, \tag{16}$$

where Q_k and F_k are the Fourier transform for the k^{th} mode of the modal displacement and of the exciting force respectively.
If $\mathbf{K}_2 = \mathbf{0}_{1,2n}$, the control is called a state control and is a common approach used in (Preumont, 2001; Boutin, 2011) for example. With $\mathbf{K}_1 = (k_1^d, ..., k_n^d, k_1^v, ..., k_n^v)$, (16) becomes

$$\frac{Q_k}{F_k} = \frac{1}{((\omega_k^2 + k_k^d\Pi_k^a\Pi_k^s) - \omega^2) + j\omega(2\xi_k\omega_k + k_k^v\Pi_k^a\Pi_k^s)}. \tag{17}$$

Thus, a modification can be applied to the modal damping and to the modal frequency of each controlled mode using k_k^d and k_k^v respectively. An example is given in Figure 3. In this case, a pole placement algorithm using the eigenvalues of $(\mathbf{A} - \mathbf{B}\mathbf{K}_1)$ is convenient for choosing the new modal damping and modal frequency of the structure modes when poles of (2) are directly linked to modal parameters. Such a method allows the choice of the pole position of each mode, keeping the system theoretically stable if real parts of the poles are chosen negative. The principle is to set the conjugate poles of the system given by $p_k = -\xi_k\omega_k \pm j\omega_k\sqrt{1-\xi_k^2}$ for the k^{th} mode at desired locations. The desired characteristic polynomial is given by

$$P_d(\lambda) = \prod_{k=1}^{n}(\lambda - \lambda_k). \tag{18}$$

Moreover, the eigenvalues of the controled system are given by

$$P_c(\lambda) = det(\lambda\mathbf{Id}_{2n,2n} - (\mathbf{A} - \mathbf{B}\mathbf{K}_1)). \tag{19}$$

Then, the coefficients of the gain vector $\mathbf{K}_1$ are chosen to equalise these two characteristic polynomials.
If $\mathbf{K}_1 = \mathbf{0}_{1,2n}$, the control is called a derivative state control. This approach is not much exploited for control of vibration even if some applications can be found in (Lhuillier et al., 2008) for example. With $\mathbf{K}_2 = (k_1^v, ..., k_n^v, k_1^a, ..., k_n^a)$, (16) becomes

$$\frac{Q_k}{F_k} = \frac{1}{(\omega_k^2 - (1 + k_k^a\Pi_k^a\Pi_k^s)\omega^2) + j\omega(2\xi_k\omega_k + k_k^v\Pi_k^a\Pi_k^s)}. \tag{20}$$

Thus, the amplitudes of the controlled modes can be shifted thanks to the gain k_k^a which can control the modal mass of the k^{th} mode. In this case, a recursive pole placement algorithm (Abdelaziz and Valàšek, 2003) is convenient for finding the gain vector $\mathbf{K}_2$, keeping the system theoretically stable if real parts of the poles are chosen negative. Thus, $\mathbf{K}_2$ is obtained with

$$\mathbf{K}_2 = \frac{det\,(-\mathbf{A})}{\prod_{k=1}^{n} -\lambda_k}\mathbf{p}_n', \tag{21}$$

where λ_k $(k = 1, ..., n)$ is the set of desired eigenvalues and $\mathbf{p}'_n$ is defined so that

$$\mathbf{p}'_0 = \mathbf{p}_1\mathbf{A}^{-1} = \mathbf{e}_n^t\,(\mathbf{AR})^{-1}\,,\ \mathbf{p}'_k = \mathbf{p}'_{k-1}\,(\mathbf{A} - \lambda_k\mathbf{Id}_n)\,,\ k = 1, ..., n, \tag{22}$$

where $\mathbf{R} = (\mathbf{B}\quad \mathbf{AB}\quad \mathbf{A}^2\mathbf{B}\,...\,\mathbf{A}^{n-1}\mathbf{B})$ is the controllability matrix, $\mathbf{e}_n = [0, ..., 0, 1]^t$ and $\mathbf{p}_1 = \mathbf{e}_n^t\,\mathbf{R}^{-1}$. This pole placement algorithm can be applied and ensure the stability of the system only if the necessary and sufficient conditions are provided. These conditions are given in (Abdelaziz and Valàšek, 2003). The first one is that the term $det(-A)$ in (21) must be non-zero. This condition is provided directly by the modelisation of the structure. The second one is that the controllability matrix R must be full rank. However, it may be noted that the acceleration term k_k^a also changes both the modal damping and modal frequency of the k^{th} mode as it is shown in Figure 3. To change just the amplitude of a mode three gains are needed.
If state and derivative state control are combined, which means that the control signal is given by (15) with $\mathbf{K}_1 \neq \mathbf{0}_{1,2n}$ and $\mathbf{K}_2 \neq \mathbf{0}_{1,2n}$, (16) becomes

$$\frac{Q_k}{F_k} = \frac{1}{((\omega_k^2 + k_k^d\Pi_k^a\Pi_k^s) - (1 + k_k^a\Pi_k^a\Pi_k^s)\omega^2) + j\omega(2\xi_k\omega_k + k_k^v\Pi_k^a\Pi_k^s)}. \tag{23}$$

Using appropriate relations between the three gains, the amplitude of the k^{th} mode can be increased or decreased. In this case, a double pole placement is necessary to ensure the theoretical stability of a n modes system. The first pole placement using a recursive algorithm gives the gain vector $\mathbf{K}_2$. Then, a usual pole placement method is used to determine the gain vector $\mathbf{K}_1$. Because of the first pole placement, $\mathbf{K}_2$ is now considered to be a fixed parameter. The second pole placement is not done with the eigenvalues of $(\mathbf{A} - \mathbf{BK}_1)$ but with those of $((\mathbf{Id}_{2n,2n} + \mathbf{BK}_2)^{-1}(\mathbf{A} - \mathbf{BK}_1))$ with the condition that the matrix $(\mathbf{Id}_{2n,2n} + \mathbf{BK}_2)$ is non-singular. The first pole placement changes the mode's amplitude but also its damping and frequency. Thanks to the second pole placement, it is possible to set these two last values to open loop damping and frequency. Hence, mode amplitude changes while damping and frequency stay the same. Figure 3 shows an example of the simulated amplitude of one mode after this double pole placement.

[Figure 3 about here.]

The results with $\mathbf{K}_2 = \mathbf{0}_{1,2n}$ and $\mathbf{K}_1 = \mathbf{0}_{1,2n}$ are also presented in Figure 3. In the first case, the frequency and the damping of the mode are effectively modified. In the second case, the frequency and the damping of the mode are also modified. Due to the damping change, it is hard to identify the influence of the amplitude modification imposed by the gain k_k^a of (17). These two controls have to be combined to enable the amplitude control without changing the frequency and the damping of the mode.
However, it must be noted that modal active control isn't an independent control. This means that the control of one mode could affect other modes. The vector $\mathbf{B}$ terms can't be chosen and depend on the features and location of actuators. So the effect of one mode control has consequences on the other modes. In the case of experimental structure, each $\mathbf{B}$ term is different and so the modification in amplitude for each mode should be different too. This phenomenon is presented in a next section.

2.3.2 Design of the observer

The controller of (15) needs the modal derivative state and the modal state of the structure as its input. An observer described by (24) is introduced in the feedback loop to estimate this modal states.

$$\begin{cases} \dot{\hat{\mathbf{X}}}(t) = \mathbf{A}\hat{\mathbf{X}}(t) + \mathbf{B}u(t) + \mathbf{L}(y(t) - \hat{y}(t)) \\ \hat{y}(t) = \mathbf{C}\hat{\mathbf{X}}(t) \end{cases} . \tag{24}$$

Then (15) becomes

$$u(t) = -\mathbf{K}_1\hat{\mathbf{X}}(t) - \mathbf{K}_2\dot{\hat{\mathbf{X}}}(t). \tag{25}$$

The matrix $\mathbf{L}$ determines the convergence properties of the control system and can be calculated thanks to a linear quadratic estimator (LQE) algorithm. The principle of this method is to minimise a cost function including two terms. The first one is related to the speed and the second to the precision of the observer. A compromise between these two properties has to be made choosing the coefficient applied on each term.
In the next section, the control method described earlier is simulated on an experimental setup.

3 Control application on a simplified active soundboard

In this section, the proposed method described in section 2 is applied to a model built with data from the experimental setup. Then, the effects of this combined control method are simulated and described.

3.1 The experimental setup

Figure 4 presents the experimental setup. It consists of a rectangular spruce plate identical to those used by string instrument makers to make musical instrument soundboards. Its edges are under clamped boundary conditions. Its dimensions are given in Table 1.

[Figure 4 about here.]

[Table 1 about here.]

A single string is tied on and connected to the bridge almost parallel with the soundboard plane. Its tension is chosen to set the fundamental frequency of the note at approximately 75 Hz. This frequency choice is explained in section 3.2. This simplified instrument is chosen for several reasons. The first one is that the usual monochord is not adapted to this study. Indeed, a soundboard is needed to modify the sound of the controlled instrument. The second one is that a string instrument is too complex to easily study the control effect on its sound. The transducers are piezoelectric patches made in PZT-5H. Their dimensions are given in Table 1. For each of the two positions shown in Figure 4, four patches are bonded side by side. The choice of this position is explained in section 3.2. The characteristics of the wood are given in Table 2 (Guitard, 1987). Those of the piezoelectric material are given in Table 3.

[Table 2 about here.]

[Table 3 about here.]

In this first study, only two piezoelectric transducers are used. The first one, located in the bottom left quarter of the plate in Figure 4, is used as the actuator in the control system. The second one, located in the top right quarter of the plate in Figure 4, is used as the sensor.

3.2 Choice of the control target

The aim of this study is to modify the sound of this simple string instrument. As previously states, one of the possible basic ways of modeling a bowed string instrument is to consider that the harmonic string signal is filtered by the Frequency Response Function (FRF) at the bridge of the soundboard. Then this signal is radiated by the soundboard, giving the instrument sound. According to this simple modeling, the modification of the soundboard's modal parameters has an effect on the radiated sound. The control of the soundboard can modify both the sound level and the timbre of the bowed string instruments if it is applied to specific modes. The string signal has to be taken into account if one wants the control to have a maximum effect. For a bowed string signal the string partials are harmonic. As the first mode of vibration of the soundboard is approxymately at 73 Hz, the fundamental frequency of the string signal is chosen to roughly match 75 Hz as shown in Figure 5. Hence, the control of the first soundboard mode can modify the amplitude of the first harmonic of the string signal. In order to limit the number of modes to control, only the first, the second, the third and the fifth harmonics are chosen to be modified. It can be noted that these harmonics are the fundamental, the octave, the fifth (plus one octave) and the third (plus two octaves) respectively.

[Figure 5 about here.]

In order to modify the second, third and fifth harmonics, other soundboard modes have to be controlled. A modal analysis is conducted on the experimental setup to find its modal parameters thanks to an Advanced Linear Curve Fitting (ALCF) algorithm. Vibration measurements are used to estimate the modal frequencies, damping and the modal shape of the structure. In our case, FRF between an impact hammer and a laser vibrometer have been used. The Table 4 gives the frequencies of the first ten modes of the soundboard.

[Table 4 about here.]

The modes whose frequency approximately matches the frequency of the harmonics given in Table 5 are the modes to control. Their numbers are given opposite the harmonics they are able to modify.

[Table 5 about here.]

To ensure the maximum control effect on each mode, the location of the transducers have to be chosen carefully. The next section deals with this topic by briefly describing the used method.

3.3 Choice and placement of the transducers

Piezoelectric patches are used as transducers in this study for several reasons. Firstly, the piezoelectric patches are not very invasive. According to Table 2, the dimensions of the transducers are small. This enables to control the structure, underestimating the additional mass of the transducers. Secondly, the piezo patches can be used as sensors as well as actuators. This allows to have several configurations for the control system. An important characteristic related to transducers is their location on the soundboard. Indeed, to control specific modes, the actuator and the sensor have to be placed to have a good effect on the desired modes without exciting too much the uncontrolled modes. To reach this goal, a numerical study is

conducted. Its results are then used to find the optimal position for the transducers. The electromechanical coupling coefficient governs the energy transformation properties of one piezoelectric patch set on the soundboard. To correctly control a mode, the optimal position for transducers is given by the maximum value of the electromechanical coupling coefficient. Its expression defined in (Hagood and von Flotow, 1991) for the k^{th} mode of vibration is given by

$$k_k^2 = \frac{f_{k,co}^2 - f_{k,cc}^2}{f_{k,cc}^2}, \tag{26}$$

where $f_{k,co}$ and $f_{k,cc}$ are the frequencies of the k^{th} mode of the structure when the piezoelectric patch is in open and in short circuit respectively. To find the values of this coupling coefficient on the soundboard, a numerical model built using the finite element method integrating piezoelectric patches is used. The soundboard and the piezoelectric patches are modeled using the characteristics presented in Table 2 and 3 and the coupling coefficients are calculated thanks to (26). Then, the Hać and Liu criterion gives the optimal position of the transducers when several modes have to be controlled. Thanks to the Performance Index, this criterion takes into account the optimal transducers' position to control the desired modes but also the optimal transducers' position to not excite the uncontrolled ones. This Performance Index is calculated for each position of the piezoelectric patch on the soundboard. Finally, the optimal position of the transducers is given by the location of its maximum value. This criterion is then applied in order to control modes of Table 5 and gives the location chosen in Figure 4. In the next section, the identification step described in section 2.2 is applied to find the modeling structure matrices.

3.4 Identification and modeling of the active structure

Prior to the control implementation, the RFP algorithm is used to identify the structure modal parameters. The frequency response function (o) shown in Figure 6 is used to find the state matrices. It is obtained measuring the transfer function between the actuator and the sensor piezoelectric patches. The excitation signal sent to the actuator is a chirp signal from 20 to 1600 Hz, with a 22050 Hz sampling rate.

[Figure 6 about here.]

This transfer function is used to find the estimated FRF given by (7) thanks to the RFP algorithm. 20 modes are used for the identification but only 12 are kept for the modal reconstruction. The frequencies of the ten first modes are given in Table 4. The representation of the modal model given by (8) is represented in full line (—) in the Figure 6. The FRF of the state space model after the approximation of (13) and after having kept the 12 available identified modes whose numbers are indicated by arrows in Figure 6 is represented in dashed line (**- - -**). It can be noted that the frequency, damping and amplitude of each mode correspond closely. The first peak at approximately 30 Hz is a low frequency artefact due to noise. It is therefore not used in the state space FRF model. Moreover, the decrease of gain in the high frequencies might be due to the fact that higher modes are not used for the identification. This first identification step allows the setting of matrices $\mathbf{A}$, $\mathbf{B}$ and $\mathbf{C}$. However, the matrix $\mathbf{G}$, which matches the characteristics of the disturbance location, still remains unknown. A second identification step has to be conducted to find this last matrix on a different measured FRF. It uses the bridge admittance which is another FRF measured between the bridge and the piezoelectric sensor patch using an impact hammer.

3.5 Design of the control system

The next step for the control system design is to set the gain vectors $\mathbf{K}_1$, $\mathbf{K}_2$ and $\mathbf{L}$. Transfer functions of the simulated structure for two different control configurations are presented in Figure 7. The first control configuration changes only the global gain value of the soundboard FRF. The first pole placement giving $\mathbf{K}_2$ is selected to modify the imaginary parts of the poles of modes 10 and 11 by about 40 %. The second pole placement giving $\mathbf{K}_1$ is useful for maintaining the same modal frequency and damping as in the uncontrolled structure. Figure 7(a) gives the uncontrolled FRF (—) and the controlled FRF (- - -) for this first control configuration. The second control configuration changes not only the global gain value of the soundboard FRF but also three modal frequencies and one modal damping. The first pole placement giving $\mathbf{K}_2$ remains the same while the second pole placement giving $\mathbf{K}_1$ is chosen to apply the modifications of Table 6. Figure 7(b) gives the uncontrolled FRF (—) and the controlled FRF (- - -) for this second control configuration.

[Table 6 about here.]

In the Figure 7 the arrows indicate the frequency of the harmonics of the string's force signal used in this study. It may be noted that several modes are missing from the soundboard FRF. For example modes 4 or 6 which were identified in section 3.4 are not visible here. This is due to the choice of actuator and sensor locations described in section 3.1.

[Figure 7 about here.]

Figure 7(a) shows that the combined control increases the global gain of the soundboard FRF. However, the gain increase is not equal for each mode. This is due to the fact that the modal control is not an independent control and that the coefficients of the $\mathbf{B}$ and $\mathbf{C}$ matrices depend on the features and location of the actuator and sensor. For the second control configuration shown in the Figure 7(b), modifications are selected to modify the harmonics of the string signal given in the Table 5. The frequency shifts of the first, second and ninth modes have been chosen to increase the first, second and fifth partial amplitudes respectively. The decrease of the fifth mode damping has been chosen to decrease the amplitude of the third harmonic.
The different control configurations on the soundboard model are finally presented in the next section.

4 Time simulations

The effects of the combined control applied on a soundboard model are studied in this section. A modeling software is used to build the numerical model thanks to the $\mathbf{A}$, $\mathbf{B}$, $\mathbf{C}$ and $\mathbf{G}$ matrices found in section 3.4. Then, the matrices $\mathbf{A}$, $\mathbf{B}$ and $\mathbf{C}$ and the gain vectors $\mathbf{K}_1$, $\mathbf{K}_2$ and $\mathbf{L}$ are used to build the numerical control system. It may be noted that these last numerical blocks could be used in an experimental case without any changes. The disturbance signal used in the simulation is a recording of a bowed string's force signal measured thanks to a piezoelectric sensor set under the string on a cello bridge. It is given in Figure 8(a). Then, a time simulation is conducted sending this measured time signal in the controlled soundboard model. This signal, filtered by the soundboard model, is given in Figure 8(b). It matches the simulated vibration of the soundboard measured by the piezoelectric sensor and without control of the structure. It can be noted that this second signal is smoother than the excitation signal. This is due to the fact that the soundboard model stops at approximatively 500 Hz. The high frequencies of the measured signal are filtered.

[Figure 8 about here.]

It is then possible to measure this signal for each control configuration given in Figure 7. In these cases, the shape of the signal curves is very similar to the shape of the curve of Figure 8(b) but with a larger amplitude. This means that these two control configurations make the sound louder while remaining stable thanks to the double pole placement described in section 2.3.1. Figure 9 shows the modulus of the Fourier transform of the signal as a sum of harmonic peaks whose amplitude is filtered by the uncontrolled soundboard FRF and its shape (—).

[Figure 9 about here.]

Figure 9(a) gives the Fourier transform shape of the resulting sound (- - -) for the first control configuration. This control increases the amplitude of the global soundboard FRF. The amplitude increase of each peak is given in Table 7.

[Table 7 about here.]

As mentioned in section 3.5, the amplitude increase is not equal for each peak, particularly for the fourth partial. This is not very problematic since it is not the most perceptible partial. Figure 9(b), gives the Fourier transform shape of the resulting sound (- - -) for the second control configuration. The amplitude increase in each peak and the amplitude difference between the two control configurations are given in Table 8.

[Table 8 about here.]

The effects of the frequency shifts are very clear. Indeed, partials 1, 2 and 5 increase approximately about ten decibels. The effects of damping control on the fifth mode are less clear. Even if the effect on the FRF in Figure 7 is very visible, it is too localised to impact upon the sound partial. However, a modification of the frequency with the damping control should enable the decrease of this partial. It can be noted that the frequency and damping control have an effect on the entire soundboard FRF since the amplitude of the partials 4 and 6 have also changed. So this second control configuration not only enables a change in the amplitude of the measured signal but also the modification of its timbre thanks to the changes in the frequency and damping of the modes.

5 Discussion

A first comment pertains to the stability of the control system. Using the proposed double pole placement method ensures the theoretical stability. This is achieved if the conditions given in (Abdelaziz and Valàšek, 2003) are met. However, with time simulations or experimental controls, errors can make the control system unstable. For example, estimation error of the state vector or the slowness of the observer can cause instabilities. An other example is the well-known spillover effect which makes the system unstable due to unmodeled modes in the control bandwidth.

An other comment is that this combined control method has to be tested on an experimental structure. In this case, the amplitude of the command signal must not be too high in order to keep a reasonable voltage level at the amplifier output. Thanks to the time simulations, it is possible to observe the control signal amplitude. For the first control configuration, this amplitude is near to 300 V for its highest value. This is an acceptable value since the voltage amplifier used in this control system is able to deliver a maximum value of 350 V. However,

for the second control configuration, this amplitude is near to 500 V. It is to high for the amplifier. The control signal will be saturated and the control system will not reach the control target. Modifications on the soundboard FRF have to be smaller. Which leads to the second comment. It is difficult to accurately set small amplitude modifications of the soundboard FRF since the influence of the modes on each other seems to be important. This leads to non realistic control results and could be due to the fact that a single-input/single-output (SISO) system has been used in this study. Indeed, a one sensor and one actuator system is not able to control a lot of modes at the same time. Understanding of this phenomenon, modeling of higher modes and the use of a multi-input/multi-output (MIMO) system could be a promising area of investigation.
Moreover, recent investigations have revealed that for complex structures with a large number of degrees of freedom, the values in the state matrices present a very large dynamic. This is particularly true for the structure matrix $\mathbf{A}$. This provides ill-conditionned matrices and makes impossible the computation of precise controller and observer gain vectors. Indeed, the condition given in the section 2.3.1 on the controllability matrix R is not true. This has led authors to investigate a dimensionless approach to adapt the dynamic of the state matrices. Using this method, experimental results have been obtained and should be presented in a future paper.

6 Summary

This paper proposes an approach using combined control method, enabling the change of the modal frequencies, dampings and amplitudes of a structure ensuring the stability of the system. An approach is proposed to design a control system using experimental data. The effects of this new control method are studied thanks to a time simulations on a simplified soundboard model. The result of a first simulation shows that the combined control method enables the change in the modal amplitudes of the soundboard FRF. A second simulation shows that, in addition to this first modification, the modal frequencies and dampings can be shifted independently. Applied to musical instruments, this combined control method allows the modification of their timbres as well as making their sound louder.

Acknowledgments

This work has been done during the PhD of Simon Benacchio, funded by the Agence National de la Recherche (ANR IMAREV project). The authors would like to thank René Caussé and Alain Terrier.

References

Abdelaziz, T. (2012), 'Parametric eigenstructure assignement using state-derivative feedback for linear systems', *Journal of Vibration and Control* **18**(12), 1809–1827.

Abdelaziz, T. and Valàšek, M. (2003), 'A direct algorithm for pole placement by state-derivative feedback for single-input linear systems', *Acta Polytechnica* **43**(6), 52–60.

Benacchio, S., Mamou-Mani, A., Chomette, B. and Ollivier, F. (2013), Modal active control applied to simplified string musical instrument, *in* 'Proc. Int. Conf. of Acoustics', Montréal, Canada.

Berdahl, E. and Smith III, J. (2007), Inducing unusual dynamics in acoustic musical instruments, *in* 'IEEE International Conference on Control Applications, CCA 2007', Singapore, pp. 1336–1341.

Berdahl, E., Smith III, J. and Freed, A. (2006), Active damping of a vibrating string, *in* 'Active 2006', Adelaide, Australia.

Boutin, H. (2011), Méthodes de contrôle actif d'instruments de musiques acoustiques, PhD thesis, Université Pierre et Marie Curie.

Boutin, H. and Besnainou, C. (2012), A modal method adapted to the active control of a xylophone bar, *in* 'Proc. Acoustics 2012', Nantes, France.

Chesné, S., Jean-Mistral, C. and Gaudiller, L. (2013), 'Experimental identification of smart material coupling effects in composite structures', *Smart Material and Structures* **22**(7), 1–10.

Chomette, B., Remond, D., Chesné, S. and Gaudiller, L. (2008), 'Semi-adaptive modal control of on-board electronic boards using identification method', *Smart Material and Structures* **17**, 1–8.

Dai, L. (1989), *Singular control systems*, Springer Ed.

Franklin, G., Powell, J. and Emami-Naeini, A. (1994), *Feedback control of dynamic systems*, Addison Wesley.

Fuller, C., Elliott, S. and Nelson, P. (1996), *Active control of vibration*, Academic Press.

Gawronski, W. (1998), *Dynamics and control of structures, A modal approach*, Springer Ed.

Griffin, S. (1995), Acoustic replication in smart structures using active structural/acoustic control, PhD thesis, Georgia Institute of Technology.

Guitard, D. (1987), *Mécanique du matériau bois et composites*, CEPADUES Ed.

Hać, A. and Liu, L. (1993), 'Sensor and actuator location in motion control of flexible structures', *Journal of Sound and Vibration* **167**(2), 239–261.

Hagood, N. and von Flotow, A. (1991), 'Damping of structural vibrations with piezoelectric materials and passive electrical networks', *Journal of Sound and Vibration* **146**(2), 243–268.

Jansson, E. (2002), *Acoustics for violin and guitar makers*, TMH, Speech, Music and Hearing.

Lhuillier, V., Gaudiller, L., Pezerat, C. and Chesné, S. (2008), 'Improvement of transmission loss using active control with virtual modal mass', *Advances in Acoustics and Vibration* pp. 1–9.

Luenberger, D. (1971), 'An introduction to observers', *IEEE Transactions on Automatic Control* **16**(6), 596–602.

Mathews, M. and Kohut, J. (1973), 'Electronic simulation of violin resonances', *Journal of the Acoustical Society of America* **53**(6), 1620–1626.

Meirovitch, L. (1990), *Dynamics and control of structures*, John Wiley and Sons.

Nelson, P. and Elliott, S. (1992), *Active control of sound*, Academic Press.

Piefort, V. and Preumont, A. (2000), Modeling of smart piezoelectric shell with finite elements, *in* 'Proc. ISMA 25', Leuven, Belgium.

Preumont, A. (2001), *Vibration control of active structures: An introduction*, Spinger Ed.

Richards, R. (1979), *An introduction to dynamics and control*, Longman.

Richardson, B. (2002), 'Simple models as basis for guitar design', *Journal Catgut Acoustical Society* **4**, 30–36.

Richardson, M. and Formenti, D. (1982), Parameter estimation from frequency response measurements using rational fraction polynomials, *in* 'Proc. IMAC Conference', Orlando, FL, USA.

List of Figures

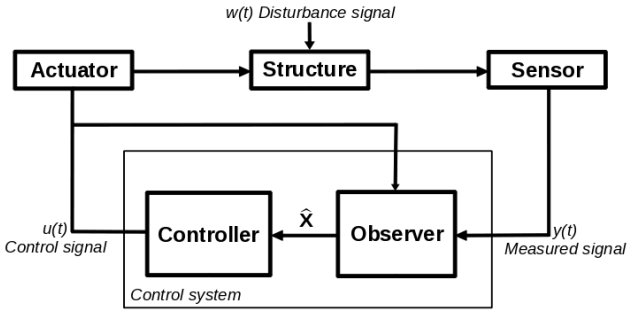

Figure 1: Modal control feedback loop.

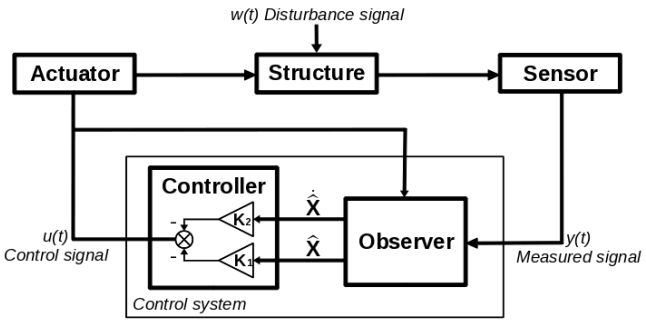

Figure 2: Combined modal control feedback loop.

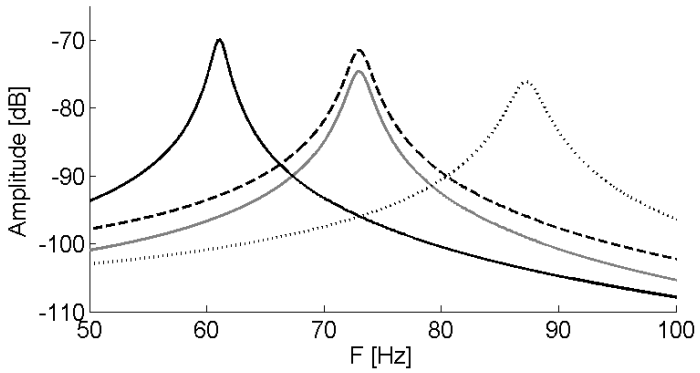

Figure 3: Amplitude of one mode without (——) and with (– – –) combined control. Results obtained with $\mathbf{K}_2 = \mathbf{0}_{1,2n}$ (——) and $\mathbf{K}_1 = \mathbf{0}_{1,2n}$ (. . . . .).

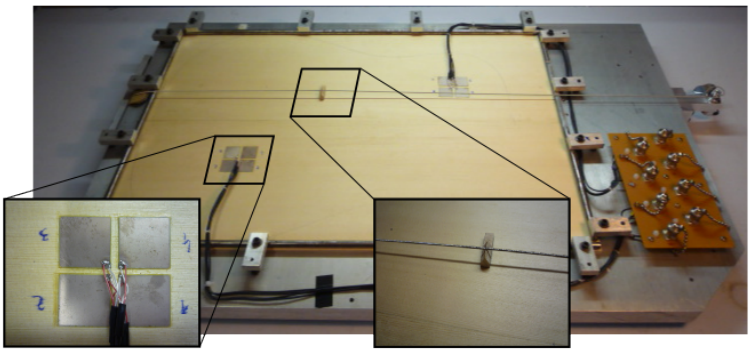

Figure 4: Experimental setup.

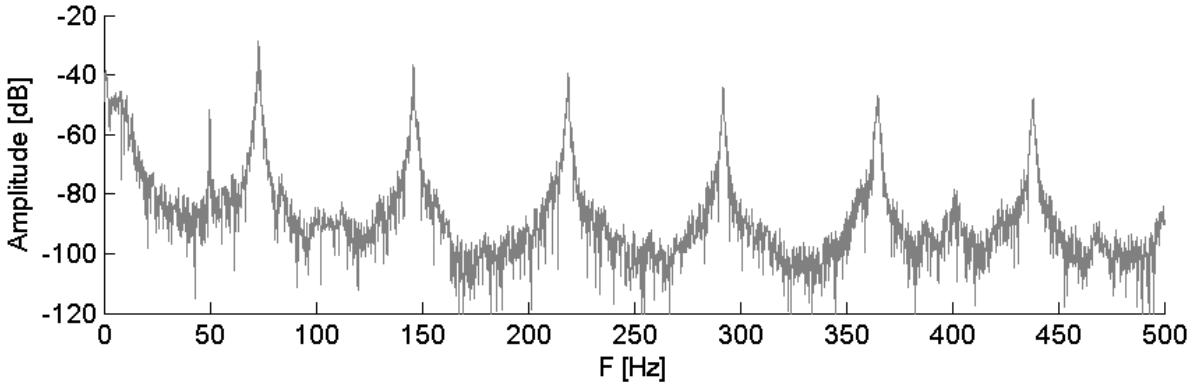

Figure 5: Fourier transform of the string signal whose fundamental frequency is approximately set to 75 Hz.

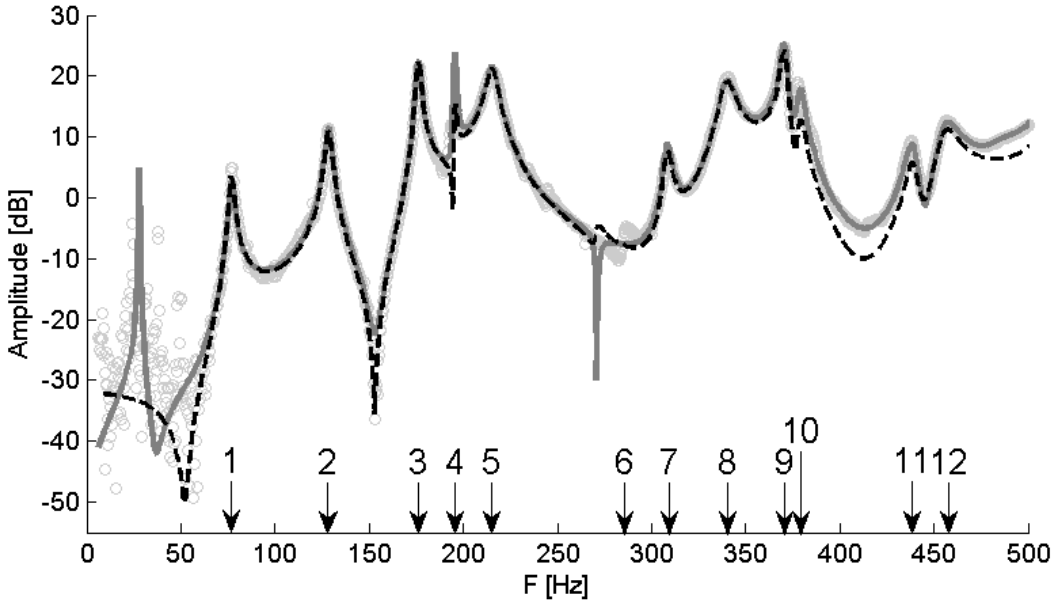

Figure 6: FRF (o), modal reconstruction (—) and state space model (- - -). Arrows indicate the modes' number.

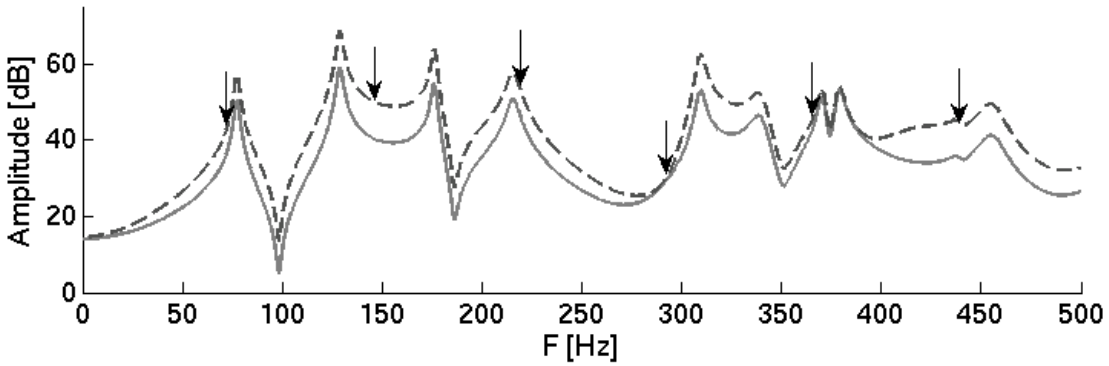

(a) Soundboard FRF without (—) and with (- - -) combined control for the first control configuration.

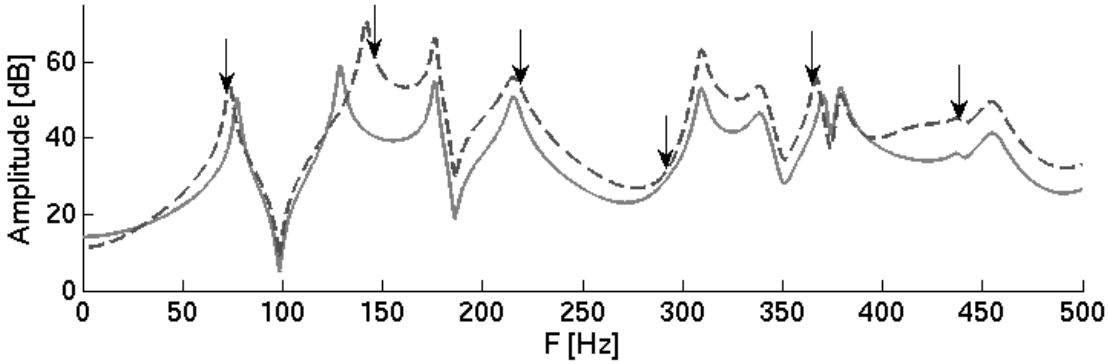

(b) Soundboard FRF without (—) and with (- - -) combined control for the second control configuration.

Figure 7: Two control configurations of the soundboard FRF.
Arrows give the partials' frequency of the string's force signal.

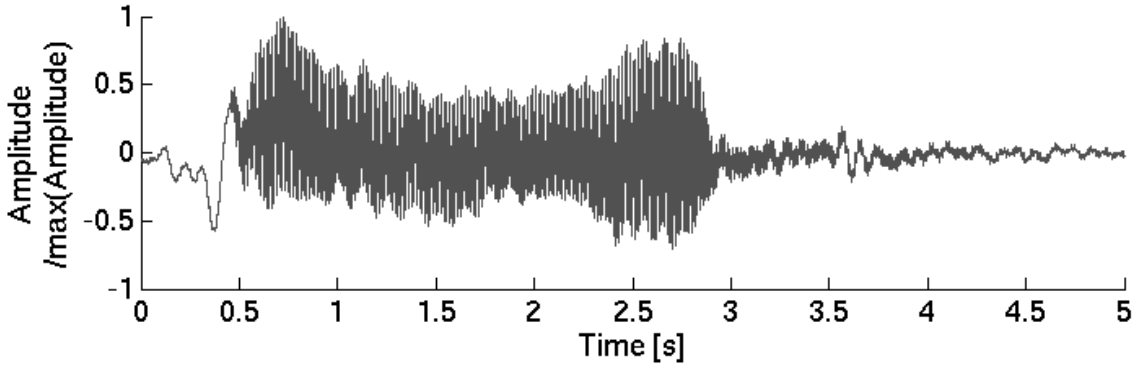

(a) String's force signal used as disturbance on the numerical soundboard model applied to the bridge location.

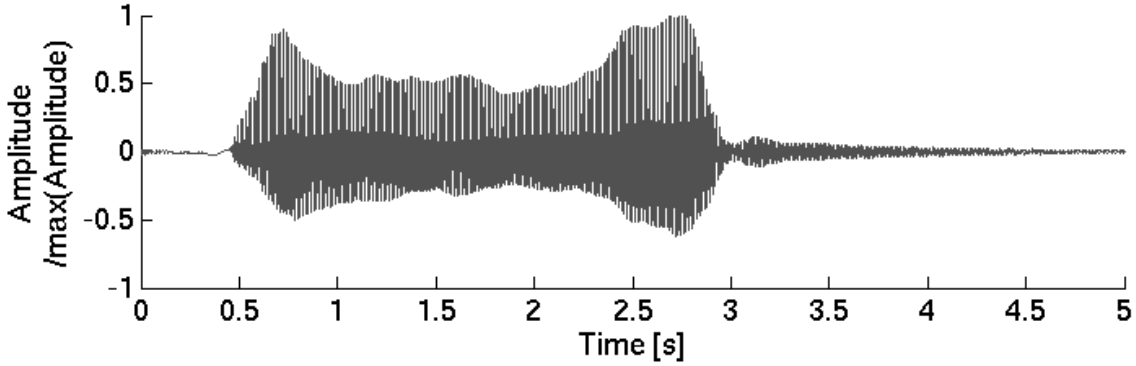

(b) Simulation given by piezoelectric sensor.

Figure 8: Excitation and measured signals.

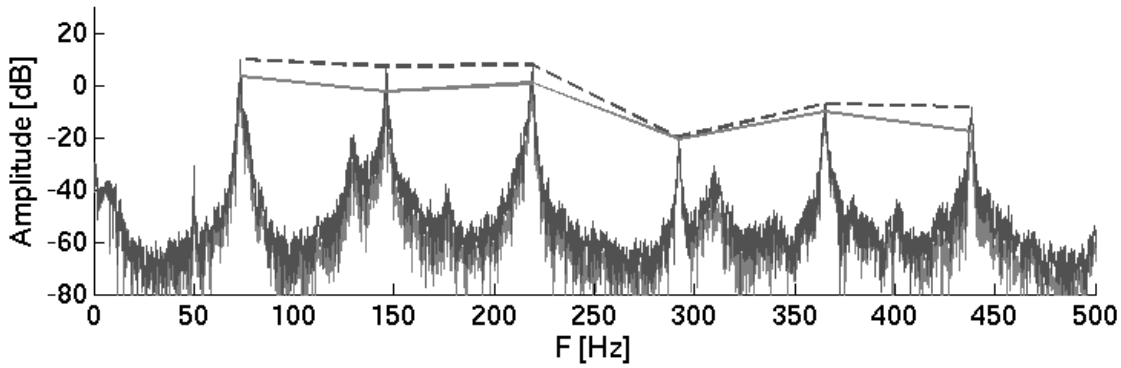

(a) Fourier transform shape of the measured signal without (—) and with (- - -) combined control for the first configuration.

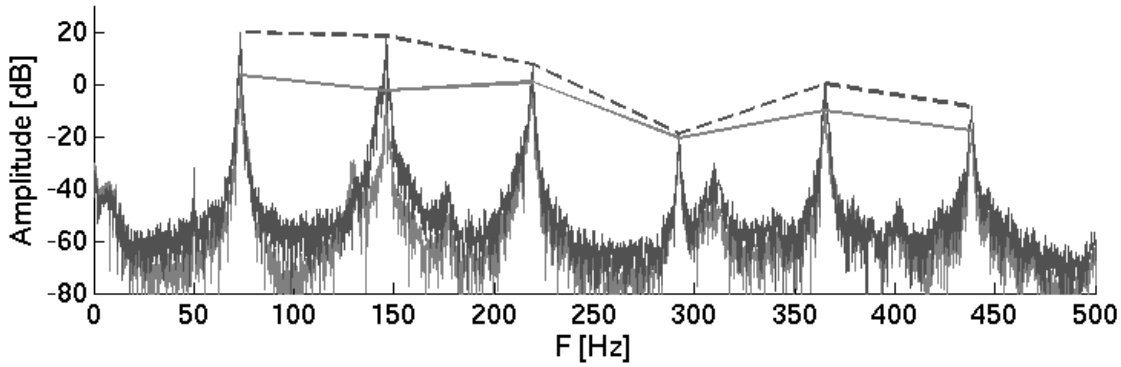

(b) Fourier transform shape of the measured signal without (—) and with (- - -) combined control for the second configuration.

Figure 9: Effects of the two control configurations on the measured signal.

List of Tables

Table 1: Plate and piezoelectric patches dimensions.

	Wide [m]	Long [m]	Thick [m]
Plate	0.4	0.6	0.004
Piezo	0.02	0.02	0.0002

Table 2: Wooden plate characteristics, with E the Young modulus, G the shear modulus, ν the Poisson coefficient and ρ the density.

E_x [GPa]	E_y, E_z [GPa]	G_{xy}, G_{xz}, G_{yz} [GPa]	$\nu_{xy}, \nu_{xz}, \nu_{yz}$	ρ [kg.m^{-3}]
11.5	0.47	0.5	0.005	392

Table 3: Elastic, piezoelectric and dielectric constants of piezoelectric materials.

c_{11}^E, c_{22}^E [GPa]	c_{33}^E [GPa]	c_{12}^E [GPa]	c_{13}^E [GPa]
127.2	117.4	802.1	846.7

e_{31} [C.m^{-2}]	e_{33} [C.m^{-2}]	e_{33}^S [nF.m^{-1}]
-6.6	23.2	8.85

Table 4: Frequencies of the first ten modes of vibration of the soundboard.

Mode	1	2	3	4	5	6	7	8	9	10
Frequency [Hz]	73	112	177	193	216	283	308	344	376	389

Table 5: Modes of vibration to control in order to modify the amplitude of string signal partials.

Harmonic	Frequency [Hz]	Mode
1 (Fundamental)	75	1
2 (Octave)	150	2
3 (Fifth)	225	5
5 (Third)	375	9 10

Table 6: Modifications applied to modes 1, 2, 5 and 9 thanks to combined control.

Mode	Frequency shift [%]	Damping shift [%]
1	-5	0
2	+10	0
5	0	-50
9	-1	0

Table 7: Partials amplitude increase for the first control configuration compared to uncontrolled configuration.

Partial	Amplitude increase [dB]
1	6.5
2	9.7
3	6.9
4	0.8
5	2.7
6	9.2

Table 8: Partials amplitude increase for the second control configuration compared to uncontrolled configuration and amplitude difference between the first and the second control configuration.

Partial	Amplitude increase [dB]	Difference [dB]
1	16	9.5
2	20.8	11.1
3	6.5	-0.4
4	2	1.2
5	10.2	7.5
6	8.9	-0.3